

Plasticity in growth behavior of patients' acute myeloid leukemia stem cells growing in mice

Resistance against chemotherapy remains a major obstacle in treating patients with acute myeloid leukemia (AML).¹ Novel therapeutic concepts are especially desired to target and eliminate resistant AML stem cells. Here we show that AML stem cells harbor plasticity, a changing pattern of biological behavior, by demonstrating that AML stem cells reversibly switch from a low-cycling, chemotherapy resistant state into an actively proliferating state associated with a response to standard chemotherapy.

We used patient-derived xenograft (PDX) cells from patients with high risk or relapsed AML that were lentivirally transduced for marker expression. We stained these cells with the proliferation-sensitive dye carboxyfluorescein succinimidyl ester (CFSE), and re-transplanted them into next-recipient mice. A rare subpopulation of AML cells displayed reduced proliferation *in vivo*, associated with resistance against standard chemotherapy. The proportion of AML cells with stem cell potential was identical in both, the high and low proliferative sub-fractions. In re-transplantation experiments, proliferation behavior proved reversible, and AML stem cells were able to switch between a high and low proliferation state. Our data indicate that AML stem cells display functional plasticity *in vivo*, which might be exploited for therapeutic purposes, to prevent AML relapse and ultimately improve the prognosis of patients with AML.

AML patients are at risk to suffer disease relapse associated with dismal prognosis. The rare subpopulation of AML stem cells (or leukemia initiating cells [LIC]) might be responsible for relapse by combining self-renewal capacity with dormancy and resistance against standard chemotherapy.² AML LIC features, including the growth phenotype, have long been considered mainly constant and persistent;²⁻⁵ in contrast, recent data suggest unsteady features under therapeutic pressure,^{6,7} while data without experimental treatment pressure remain elusive. Putative functional plasticity of AML LIC is of major clinical importance as it might enable novel therapeutic options.

We previously reported functional plasticity in acute lymphoblastic leukemia (ALL), where we showed *in vivo* that long-term dormant, treatment-resistant ALL cells were able to convert into highly proliferative, treatment-sensitive cells and *vice versa*.⁸ Nevertheless, AML and ALL differ widely regarding stem cell biology and a defined stem cell hierarchy - characteristic for AML - has not been proven in ALL. Based on diverse stem cell characteristics, we considered the functional plasticity of LIC conceivable in ALL, but hypothesized its absence in AML.

To test our hypothesis, we studied cells from ten patients with high-risk or relapsed AML of different karyotypes, genotypes and clinical histories (*Online Supplementary Table S1*). As a clinic-close model system, primary cells were transplanted into immunocompromised mice, and AML PDX models were established.⁹ PDX models were selected to allow for serial transplantation; as this ability is restricted to highly aggressive disease, our study is biased towards high risk AML. AML PDX models were genetically engineered to express luciferase for bioluminescence *in vivo* imaging and mCherry for cell enrichment by flow cytometry. Marker expression remained stable over serial re-transplantation and allowed enrichment of minute numbers of PDX AML cells from murine bone marrow (Figure 1A, for details see the *Online Supplementary Materials and Methods*). As con-

trols, three samples (AML-356, AML-358 and AML-538) were studied without prior genetic engineering.

AML PDX samples showed more than 3-fold differences in doubling times *in vivo*, resulting in variable time to overt disease in mice (*Online Supplementary Figure S1A-B*). When PDX cells were re-isolated from murine bone marrow, mCherry expression enabled unbiased enrichment of AML PDX cells, independent of other, putatively subpopulation-restricted, surface markers on AML cells (Figure 1B).^{8,10} Re-isolation of PDX cells revealed that homing was heterogeneous between samples, as 0.01-1% of PDX cells could be re-isolated from mice early after transplantation (*Online Supplementary Figure S1C*). The frequency of LIC, as determined in limiting dilution transplantation assays, varied by a factor of 10 between samples (*Online Supplementary Figure S1D* and *Online Supplementary Table S2*). Thus, our AML PDX cohort of aggressive samples displayed major functional inter-sample heterogeneity *in vivo*, reflecting the known phenotypic heterogeneity of AML.¹¹

In order to track *in vivo* proliferation of AML cells from individual samples, PDX cells were stained with CFSE, a dye that is not metabolized in eukaryotic cells, but decreases upon cell divisions, indicating proliferation.¹² CFSE records a cell's proliferative history rather than providing a snapshot of the cell's proliferative state at a given moment. CFSE content was measured by flow cytometry at different time points following injection into groups of mice.

In accordance with an increase in leukemic burden and numbers of re-isolated cells (Figures 1CD and *Online Supplementary Figure S2A*), most AML PDX cells entirely lost CFSE within days of *in vivo* growth, indicating high proliferative activity in the majority of cells (Figures 1E-F and *Online Supplementary Figure S2A*). However, a minor subpopulation of cells retained CFSE over several weeks, indicating a low-cycling, putatively dormant phenotype (Figures 1E-F and *Online Supplementary Figure S2A*). We called these cells label-retaining cells (LRC) according to the literature.⁸ LRC were found in 9 of 10 samples tested (Figures 1E-F and *Online Supplementary Figure S2A-B*). Only a single sample originating from a child with a fatal AML relapse had entirely lost the LRC population between day 7 to 15 (*Online Supplementary Figure S2C*), again highlighting the known heterogeneity of AML.¹¹ Cell cycle analysis confirmed that LRC divide less compared to non-LRC (*Online Supplementary Figure S3A*). Together, our data reveal, in the majority of cases, heterogeneity of *in vivo* growth behavior within individual AML PDX samples, including a subpopulation of low-cycling LRC. Hence, our results add an important level of phenotypic heterogeneity to AML on top of the known heterogeneity of e.g., immunophenotypes, or gene expression profiles. As a large range of AML subtypes were studied (*Online Supplementary Table S1*), the novel characteristic is not limited to a specific cytogenetic or genetic subgroup.

To further characterize attributes of LRC, gene expression analysis of 24 LRC and non-LRC samples isolated from AML-393 and AML-491 was performed.¹³ Among the top down regulated gene sets in LRC were cell cycle regulators, confirming the reduced proliferative state of these cells (*Online Supplementary Figure S3B-C*); among the top upregulated gene sets were cell adhesion molecules (*Online Supplementary Figure S3C*). Notably, LRC of AML-393 were more similar to LRC of AML-491 than to their own non-LRC (Figure 1G), despite the substantial differences in the mutational profile of AML-393 and AML-491 (*Online Supplementary Table S1*). Even more striking, gene-set enrichment analysis identified a high gene-set enrich-

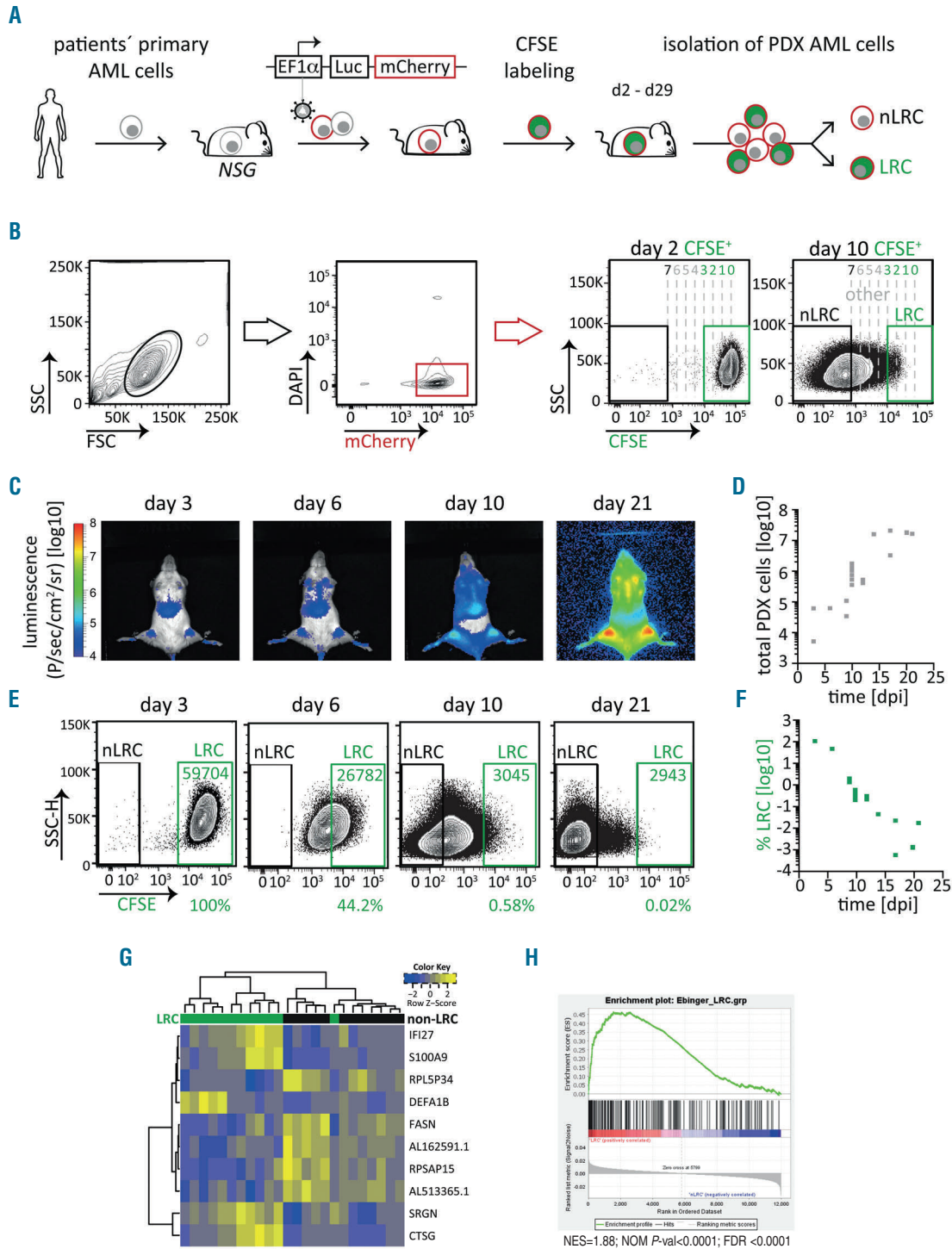


Figure 1. Acute myeloid leukemia patient-derived xenograft cells contain a rare subpopulation of low-cycling cells. (A) Experimental procedure; primary patients' acute myeloid leukemia (AML) cells were transplanted into NSG mice, resulting patient-derived xenograft (PDX) cells were genetically engineered, sorted, and amplified. At advanced disease stage, mCherry⁺ AML PDX cells were isolated, stained with carboxyfluorescein succinimidyl ester (CFSE), and re-transplanted. At different time points, AML cells were re-isolated from mouse bone marrow, enriched, and CFSE content measured by flow cytometry, to detect CFSE-positive, low-cycling label-retaining cells (LRC), and CFSE-negative, proliferating non-LRC (nLRC). NSG: NOD.Cg-Prkdcscid Il2rgtm1Wjl/SzJ; EF1 α : elongation factor 1- α promoter; Luc: enhanced firefly luciferase. (B) Gating strategy: bone marrow cells depleted of murine cells by MACS were gated on (i) leukocytes, (ii) DAPI-mCherry⁺ AML PDX cells, and (iii) separated into LRC and non-LRC according to their CFSE content. Maximum CFSE mean fluorescence intensity (MFI) was measured at day 2 after cell injection or in *in vitro* cultivation, and divided by factor 2 to model cell divisions (dotted lines); upon less than three divisions, cells were considered as low-cycling LRC, upon more than seven divisions as proliferating non-LRC; days indicate time after cell injection. (C-D) Growth of AML-393 cells monitored by *in vivo* imaging (C) or by quantifying PDX cells re-isolated from mouse bone marrow using flow cytometry (n=21) (D); each square represents data from one mouse. (E-F) A rare subpopulation of AML PDX cells retains CFSE upon prolonged *in vivo* growth. AML-393 cells from different time points in (D) were analyzed by flow cytometry for CFSE using the gating strategy described in (B); representative dot plots (E) and percentage of LRC cells among all isolated PDX cells are shown (F); each square represents data of one mouse. (G-H) Gene expression analysis of LRC and non-LRC. LRC and non-LRC were isolated from mice carrying AML-393 (n=4) or AML-491 (n=4) 10 or 14 days after cell injection, respectively, and subjected to RNA sequencing. Technical replicates were analyzed in 6 of 8 samples, resulting in a total of 24 samples analyzed. (G) Heatmap of top differentially regulated genes (false discovery rate [FDR] ≤ 0.05) between LRC (green) and nLRC (black) of AML-393 and AML-491. (H) LRC of AML-393 and AML-491 show significant overlap with the previously published LRC signature of acute lymphoblastic leukemia (ALL). See the *Online Supplementary Figure S1-S2* for additional data.

ment analysis identified a high overlap of significantly deregulated genes between AML LRC and our previously defined LRC signature in ALL8 (Figure 1H and *Online Supplementary Figure S3C*), suggesting comparable biologic processes activated in LRC of both, AML and ALL.

Given the long-known link between dormancy and chemo-resistance,¹⁴ we compared the drug response between low-cycling LRC and high-cycling non-LRC. Groups of mice engrafted with CFSE-labeled cells were treated with a chemotherapeutic regimen mimicking

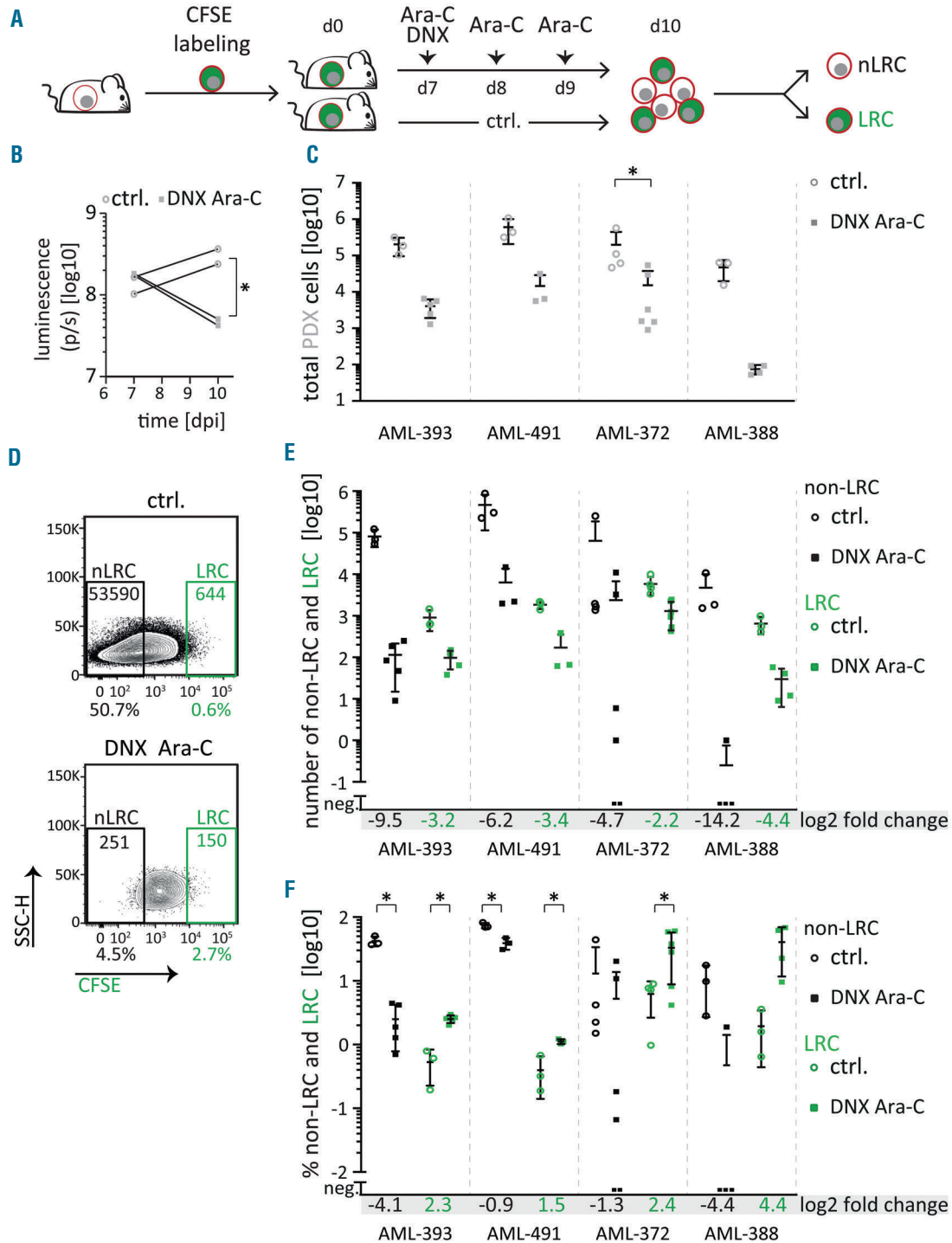


Figure 2. Low-cycling acute myeloid leukemia patient-derived xenograft cells are treatment resistant *in vivo*. (A) Experimental procedure; groups of mice were injected with carboxyfluorescein succinimidyl ester (CFSE) labeled acute myeloid leukemia patient-derived xenograft (AML-PDX) cells and treated with PBS (control [ctrl]) or a combination of 20 mg/kg DaunoXome® [DNX] on day 7 and 150 mg/kg cytarabine (Ara-C) on days 7 to 9; PDX cells were re-isolated from murine bone marrow on day 10 and analyzed as described in Figure 1B. (B) Tumor load was monitored by *in vivo* imaging in AML-393. (C) Total number of isolated PDX cells is shown of control and treated mice as mean± standard deviation (SD) of AML-393 (n=8), AML-491 (n=6), AML-372 (n=10) and AML-388 (n=7) (C); each dot/square represents one mouse. (D) Representative dot plots (AML-393). (E-F) Absolute number (E) and percentage (F) of non-label-retaining cells (non-LRC) and LRC among all isolated PDX cells are shown from the same mice as in (C); Log₂ fold reduction for each subpopulation is displayed. *P<0.05

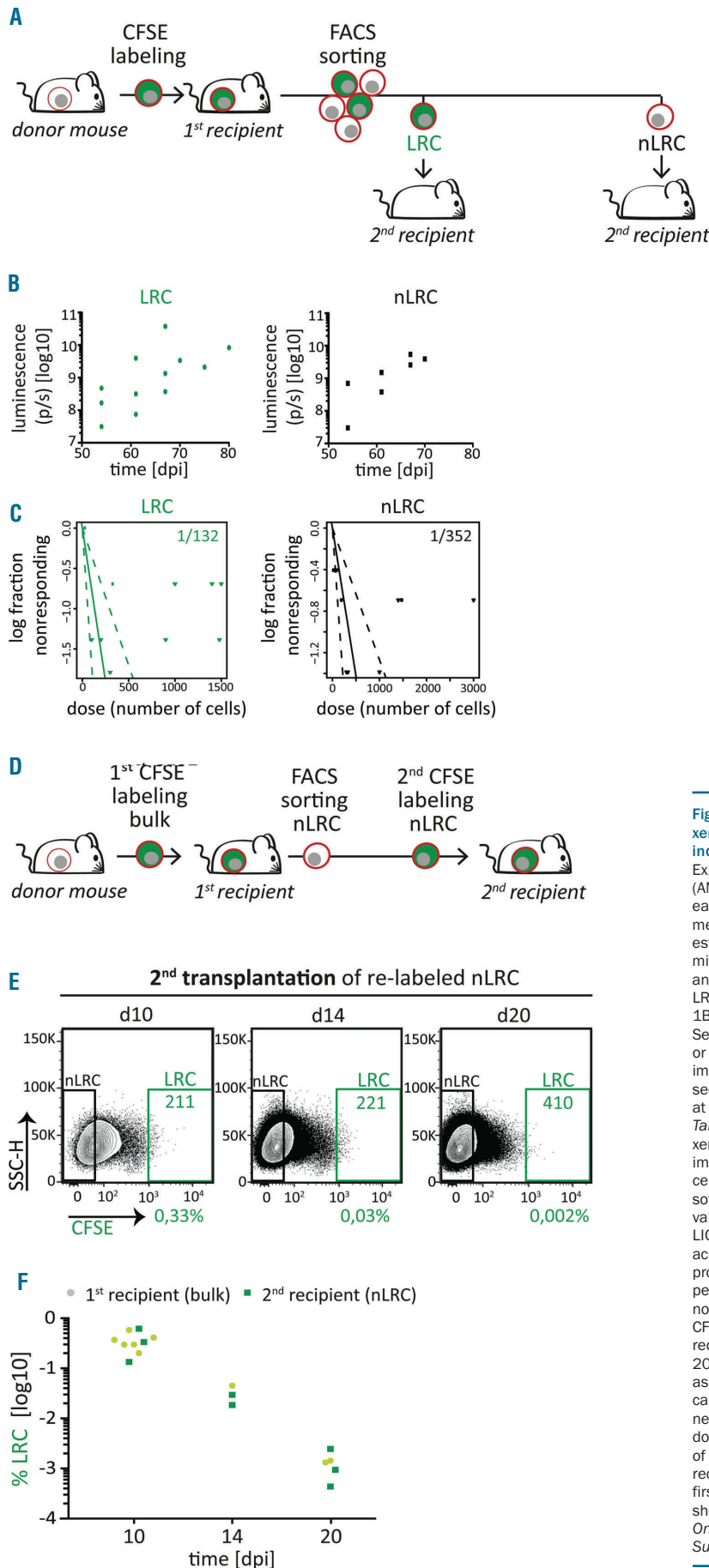


Figure 3. Acute myeloid leukemia patient-derived xenograft cells display reversible growth behavior, independently from stemness potential.

(A) Experimental procedure: acute myeloid leukemia (AML)-393 cells were isolated from advanced disease donor mice (n=5 in three independent experiments), labeled with carboxyfluorescein succinimidyl ester (CFSE), and re-transplanted into first recipient mice. Ten days after injection, cells were re-isolated and sorted into label-retaining cells (LRC) and non-LRC (nLRC) using the gates as described in Figure 1B and re-injected into secondary recipient mice. (B) Secondary recipient mice receiving either 300 LRC or 300 non-LRC (n=5) were monitored by *in vivo* imaging. (C) LRC and non-LRC were re-injected into secondary recipient mice (n=38) in limiting dilutions at numbers indicated in the *Online Supplementary Table S3*. Positive engraftment of patient-derived xenograft (PDX) cells was determined by *in vivo* imaging and/or flow cytometry. Leukemia-initiating cell (LIC) frequency was calculated using the ELDA software and is depicted +/- 95% confidence interval. No statistically significant difference between LIC frequency of LRC and non-LRC was found according to χ^2 test ($P=0.0638$). (E) Experimental procedure; from first recipient mice (n=2 in two independent experiments) harboring CFSE stained cells, non-LRC were isolated at day 21, re-stained with CFSE and 3.6×10^6 cells were injected into secondary recipients (n=8); cells were re-isolated 10, 14 and 20 days later, and LRC were quantified using gates as described in Figure 1B. The experiment is technically unfeasible for LRC as the high number of cells needed cannot be generated. (E-F) Representative dot plots (E) and quantification (F) of the percentage of LRC among all PDX cells isolated from secondary recipients is displayed (dark green squares). LRC of first recipient mice as determined in Figure 1E are shown for comparison (light green dots). See the *Online Supplementary Figure S4* and *Online Supplementary Table S3* for additional data.

"7+3" induction therapy,¹ consisting of cytarabine and liposomal daunorubicin (DaunoXome) (Figure 2A). *In vivo* treatment diminished tumor burden as monitored by *in vivo* imaging (Figure 2B), resulting in a decrease of the total isolated PDX cells by at least one order of magnitude (Figure 2C). Interestingly, while non-LRC numbers were strongly reduced by treatment, even to undetectable levels in some mice (Figures 2DE), low-cycling LRC revealed decreased sensitivity towards systemic treatment in all samples tested. As a net effect, the relative proportion of LRC was significantly enriched among cells surviving after treatment in 3 of 4 samples (Figures 2DF). Thus, low-cycling LRC show increased resistance against conventional chemotherapy *in vivo* compared to high-cycling non-LRC.

We next asked whether LRC and non-LRC differ in their ability to form tumors and performed re-transplantation experiments. Low numbers of sorted LRC and non-LRC were re-injected into secondary recipient mice in limiting dilutions close to sample-specific LIC frequency (Figures 3A and *Online Supplementary Figure S4A*). Interestingly, both, LRC and non-LRC gave rise to leukemia upon re-transplantation, indicating both subpopulations contained LIC (Figures 3B and *Online Supplementary Figure S4B*). As leukemia development was highly similar in mice transplanted with either LRC or non-LRC, low-cycling LRC must have converted into an actively proliferative state. Furthermore, we found similar LIC frequencies in LRC and non-LRC (Figure 3C, *Online Supplementary Figure S4C* and *Online Supplementary Table S3*), and no difference in CD34⁺CD38⁻ cells between the two groups (*Online Supplementary Figure S5*), strengthening previous findings.¹⁵ Notably, CD34⁺CD38⁻ cells were barely detectable in the aggressive AML-393 sample, despite the high LIC frequency (*Online Supplementary Figure S5* and *Online Supplementary Table S2*). These data indicate that LIC reside not only in the low-cycling LRC, but also in the high-cycling non-LRC compartment, indicating heterogeneity in proliferation dynamics within the AML LIC pool.

As low-cycling cells were able to convert to active proliferation, we asked whether the switch could also occur vice versa. To test whether LRC could be replenished from non-LRC, we re-transplanted high cell numbers of non-LRC retained with CFSE (Figure 3D and *Online Supplementary Figure S4D*). Upon secondary transplantation, non-LRC gave rise to a clear LRC fraction, comparable to the one from bulk cells at first transplantation, even at late time points (Figures 3E-F and *Online Supplementary Figure S4E-F*), indicating that high-cycling cells converted to a low-cycling phenotype.

These experiments revealed major functional plasticity of AML LIC phenotypes, and the ability to change their proliferation rate upon changes in external stimuli, such as re-transplantation.

Taken together, our data shows that low proliferation or dormancy characterizes a temporary, reversible cell state rather than a defined subpopulation of cells. AML contains a rare fraction of low-cycling, chemo-resistant LIC which are functionally plastic; AML LIC might temporarily adopt a low-cycling LRC phenotype or switch to a rapidly proliferating non-LRC phenotype, triggered by external stimuli such as re-transplantation. Even the highly aggressive AML samples used in this study harbor the potential to adopt a proliferative phenotype associated with response to standard chemotherapy.

Unexpectedly, we detected similar functional plasticity in AML as previously observed in ALL.⁸ This was

accompanied by similar changes in gene expression profiles, although both diseases differ substantially with regards to their stem cell biology as ALL has never revealed a stem cell hierarchy as proven in AML. In contrast to ALL, AML plasticity comes as a major surprise, as we show here that high-cycling cells harbor the potential to convert into low-cycling cells, while both populations retain stem cell capacities. In our experiments, neither functionally nor immunophenotypically defined LIC were enriched in the LRC fraction, suggesting that dormancy and stemness are not consistently linked in AML, but that dormancy characterizes a temporary cell state rather than a defined subpopulation of cells. In addition to the known constant, presumably deterministic factors defining stemness, AML stem cells appear to be regulated by additional, transient and putatively stochastic factors.¹⁶

Our data indicates that stemness and resistance to anti-leukemic therapy is not strictly linked in AML. This opens up an exciting therapeutic potential to prevent relapse and strongly supports the concept that recruiting AML LIC from their low-cycling phenotype into proliferation might sensitize them towards conventional chemotherapy.^{3,4,7} Taking advantage of the discovered heterogeneity and reversibility of the low- and high-cycling phenotypes implicates the need to identify factors responsible for AML plasticity, in addition to known microenvironment-derived regulators such as G-CSF.² The detected similarity in the transcriptome signature between LRC of AML and ALL might aid in the identification of factors that regulate these processes in both diseases. As an attractive therapeutic concept, inhibition of the reversible low-cycling state might enable to overcome treatment resistance, remove AML LIC, prevent relapse, and ultimately increase patients' prognosis.

Sarah Ebinger,¹ Christina Zeller,¹ Michela Carlet,¹ Daniela Senft,¹ Johannes W. Bagnoli,² Wen-Hsin Liu,¹ Maja Rothenberg-Thurley,³ Wolfgang Enard,² Klaus H. Metzeler,^{3,5} Tobias Herold,^{1,3,4} Karsten Spiekermann,^{3,5} Binje Vick^{1,4} and Irmela Jeremias^{1,4,6}

¹Research Unit Apoptosis in Hematopoietic Stem Cells, Helmholtz Zentrum München, German Research Center for Environmental Health (HMGU), Munich; ²Anthropology & Human Genomics, Department of Biology II, Ludwig-Maximilians-University, Martinsried, Germany; ³Laboratory for Leukemia Diagnostics, Department of Medicine III, University Hospital, Ludwig-Maximilians-University Munich, Munich; ⁴German Cancer Consortium (DKTK), partner site Munich; ⁵German Cancer Research Center (DKFZ), Heidelberg and ⁶Department of Pediatrics, Dr. von Hauner Childrens Hospital, Ludwig Maximilian University, Munich, Germany

Correspondence:
IRMEJA JEREMIAS - Irmela.Jeremias@helmholtz-muenchen.de
doi:10.3324/haematol.2019.226282

Acknowledgments: we thank Liliana Mura, Fabian Klein, Maike Frischle, Annette Frank and Miriam Krekel for excellent technical assistance; Markus Brielmeier and team (Research Unit Comparative Medicine, Helmholtz Zentrum München) for animal care services; Andreas Beyerlein (Core Facility Statistical Consulting, Institute of Computational Biology, Helmholtz Zentrum München) for assisting with statistical analysis of treatment studies; Helmut Blum and Stefan Krebs (Laboratory for Functional Genome Analysis, Gene Center, LMU, Munich) for sequencing, Claudia Baldus and Lorenz Bastian (Division of Hematology and Oncology, Charité Universitätsmedizin Berlin, Germany) for kindly providing primary cells of AML-538, and Maya C. André and Martin Ebinger (Department of Pediatric

Hematology/Oncology, University Children's Hospital Tübingen) for kindly providing pediatric AML PDX samples.

Funding: the work was supported by grants from the European Research Council Consolidator Grant 681524; a Mildred Scheel Professorship by German Cancer Aid; German Research Foundation (DFG) Collaborative Research Center 1243 "Genetic and Epigenetic Evolution of Hematopoietic Neoplasms", projects A05, A06 (to KHM), A07 (to KS) and A14 (to JWB and WE), and associate member (TH); DFG proposal MA 1876/13-1; Bettina Bräu Stiftung and Dr. Helmut Legerlotz Stiftung (all to IJ, if not indicated differently). This work was further supported by the Physician Scientists Grant (G-509200-004) from the Helmholtz Zentrum München to TH.

References

- Dohner H, Weisdorf DJ, Bloomfield CD. Acute myeloid leukemia. *N Engl J Med.* 2015;373(12):1136-1152.
- Thomas D, Majeti R. Biology and relevance of human acute myeloid leukemia stem cells. *Blood.* 2017;129(12):1577-1585.
- Ishikawa F, Yoshida S, Saito Y, et al. Chemotherapy-resistant human AML stem cells home to and engraft within the bone-marrow endosteal region. *Nat Biotechnol.* 2007;25(11):1315-1321.
- Saito Y, Uchida N, Tanaka S, et al. Induction of cell cycle entry eliminates human leukemia stem cells in a mouse model of AML. *Nat Biotechnol.* 2010;28(3):275-280.
- Hope KJ, Jin L, Dick JE. Acute myeloid leukemia originates from a hierarchy of leukemic stem cell classes that differ in self-renewal capacity. *Nat Immunol.* 2004;5(7):738-743.
- Farge T, Saland E, de Toni F, et al. Chemotherapy-resistant human acute myeloid leukemia cells are not enriched for leukemic stem cells but require oxidative metabolism. *Cancer Discov.* 2017;7(7):716-735.
- Boyd AL, Aslostovar L, Reid J, et al. Identification of chemotherapy-induced leukemic-regenerating cells reveals a transient vulnerability of human AML recurrence. *Cancer Cell.* 2018; 34(3):483-498.e5.
- Ebinger S, Ozdemir EZ, Ziegenhain C, et al. Characterization of rare, dormant, and therapy-resistant cells in acute lymphoblastic leukemia. *Cancer Cell.* 2016;30(6):849-862.
- Vick B, Rothenberg M, Sandhofer N, et al. An advanced preclinical mouse model for acute myeloid leukemia using patients' cells of various genetic subgroups and in vivo bioluminescence imaging. *PLoS One.* 2015;10(3):e0120925.
- de Boer B, Prick J, Pruis MG, et al. Prospective isolation and characterization of genetically and functionally distinct AML subclones. *Cancer Cell.* 2018;34(4):674-689.
- Arber DA, Orazi A, Hasserjian R, et al. The 2016 revision to the World Health Organization classification of myeloid neoplasms and acute leukemia. *Blood.* 2016;127(20):2391-2405.
- Takizawa H, Regoes RR, Boddupalli CS, Bonhoeffer S, Manz MG. Dynamic variation in cycling of hematopoietic stem cells in steady state and inflammation. *J Exp Med.* 2011;208(2):273-284.
- Bagnoli JW, Ziegenhain C, Janjic A, et al. Sensitive and powerful single-cell RNA sequencing using mcSCR-seq. *Nat Commun.* 2018; 9(1):2937.
- Cheung WH, Rai KR, Sawitsky A. Characteristics of cell proliferation in acute leukemia. *Cancer Res.* 1972;32(5):939-942.
- Griessinger E, Vargaftig J, Horswell S, Taussig DC, Gribben J, Bonnet D. Acute myeloid leukemia xenograft success prediction: Saving time. *Exp Hematol.* 2018;59:66-71.
- Gupta PB, Fillmore CM, Jiang G, et al. Stochastic state transitions give rise to phenotypic equilibrium in populations of cancer cells. *Cell.* 2011;146(4):633-644.